

Charge Transport Properties and Linearity of HF-CdZnTe Material

M. Bishop^{1,2*} (max.bishop@stfc.ac.uk), B. D. Cline¹, E. Gimenez³, F. K. Dejene², I. Braddock¹, J. Matheson³, M. Bettelli⁵, M. Larkin¹, M. D. Wilson¹, M. C. Veale¹, O. Fox³, S. Bugby², S. Richards¹, S. Knowles¹, S. Scully³, S. Zanettini⁴, V. Dhamgaye³

1. Introduction

As synchrotrons around the world move to Diffraction Limited Storage Rings (DLSRs) and Free Electron Lasers (FELs) upgrade to superconducting accelerators, average photon energies are planned to increase to > 12 keV and fluxes in excess of 10^6 photons·s⁻¹·mm⁻². At these photon energies, silicon detectors have a low quantum efficiency and therefore a higher Z detector material is needed. High Flux (HF) CdZnTe, produced by Redlen Technologies [4], is a promising candidate. This material has shown improved high flux capabilities compared to other variants of CdZnTe. CdZnTe has previously been unable to be used in high flux applications due to 'high flux induced polarization'. This is caused by an electric field build up in the detector due to traps [1], and has been improved with Redlen's HF-CdZnTe. This work investigates the material properties of HF-CdZnTe compared to traditional spectroscopic CdZnTe (LF-CdZnTe) [5] by performing nondestructive alpha spectroscopy, low temperature photoluminescence and beamline tests.

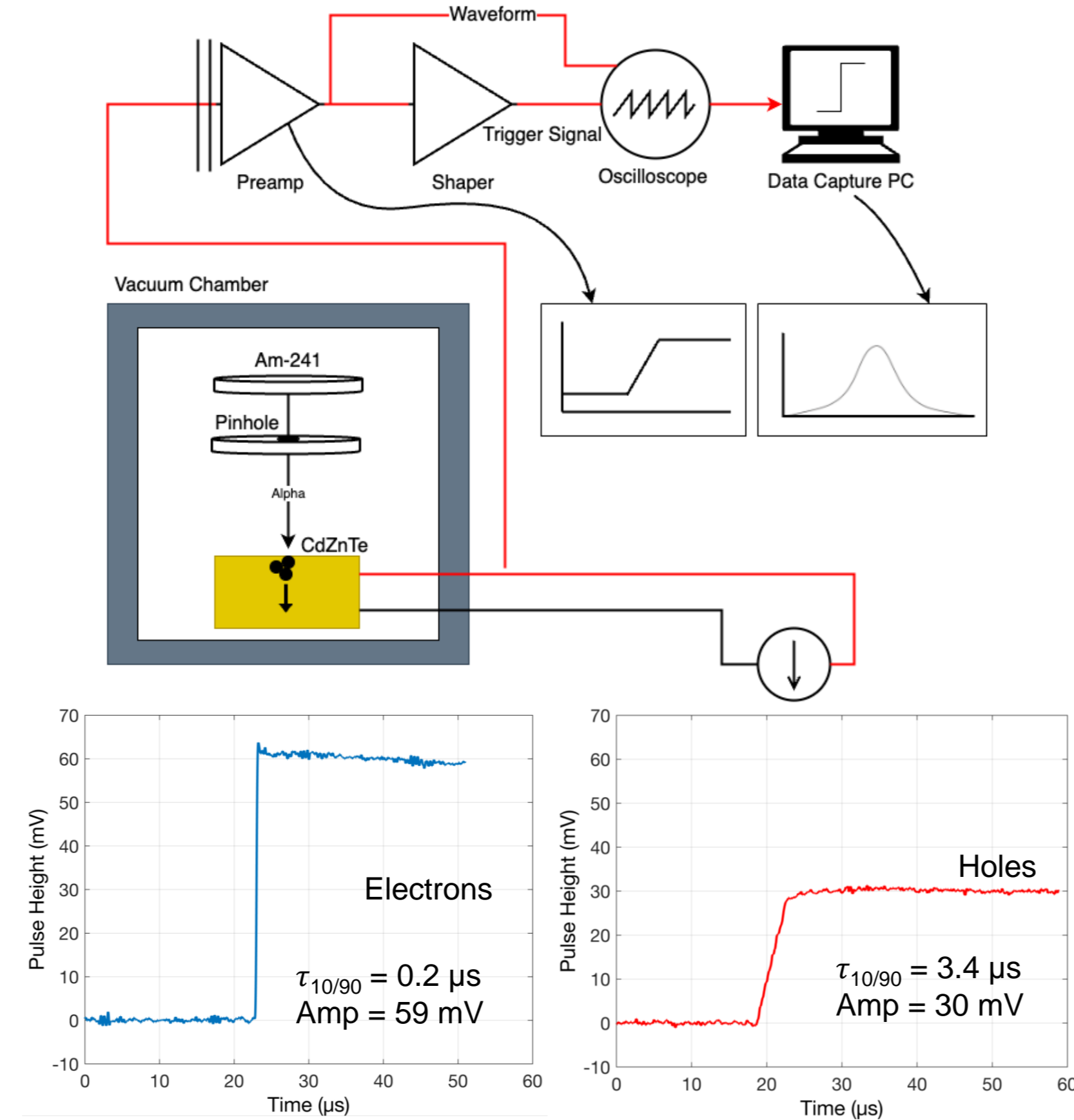


Figure 1: (Top) A schematic of the alpha spectroscopy experimental arrangement used to characterise the charge transport properties of CdZnTe. The sample is kept in a vacuum chamber with the alpha source placed 60mm and the pinhole placed at a distance 30mm from the sample. The current reading was amplified via a preamplifier and pulse shaper. (Bottom) Example of a waveforms of detector C at 200V bias. (Bottom Left) Electron pulse shape. (Bottom Right) Hole pulse shape.

2. Alpha Spectroscopy

Each detector was exposed to an americium-241 source emitting 5.48 MeV alpha radiation. These alpha particles deposit their energy in the surface of the detector. The choice of the bias voltage polarity then allows the charge transport of electrons and holes to be characterised separately. The resultant waveform was recorded by an oscilloscope shown in figure 1. The pulse height spectrum was used to find the mobility-lifetime ($\mu\tau$) via fitting the single-carrier Hecht equation, and the 10% to 90% rise time was used to find the mobility of the charge carriers.

Figure 2 & 3 show a comparison of the mobility-lifetime and mobility of 'Detector A' and 'Detector B'. These samples were fabricated in 2018 and have Redlen electrodes. This experiment was repeated for 'Detector C' and 'Detector D' which were manufactured in 2023 and have Due2lab electrodes. Table 1 shows that the charge carrier properties have been consistent over the past 5 years. Comparing the HF and LF in table 1 shows that the lifetime of holes in HF-CdZnTe is greater than in LF-CdZnTe by 2-5x, possibly causing the observed high flux improvements [1]. However, testing has shown that the electron lifetime has been reduced compared to the LF-CdZnTe.

Figure 2: Hecht fit of two 5mm thick detectors, one is HF-CdZnTe and one is LF-CdZnTe

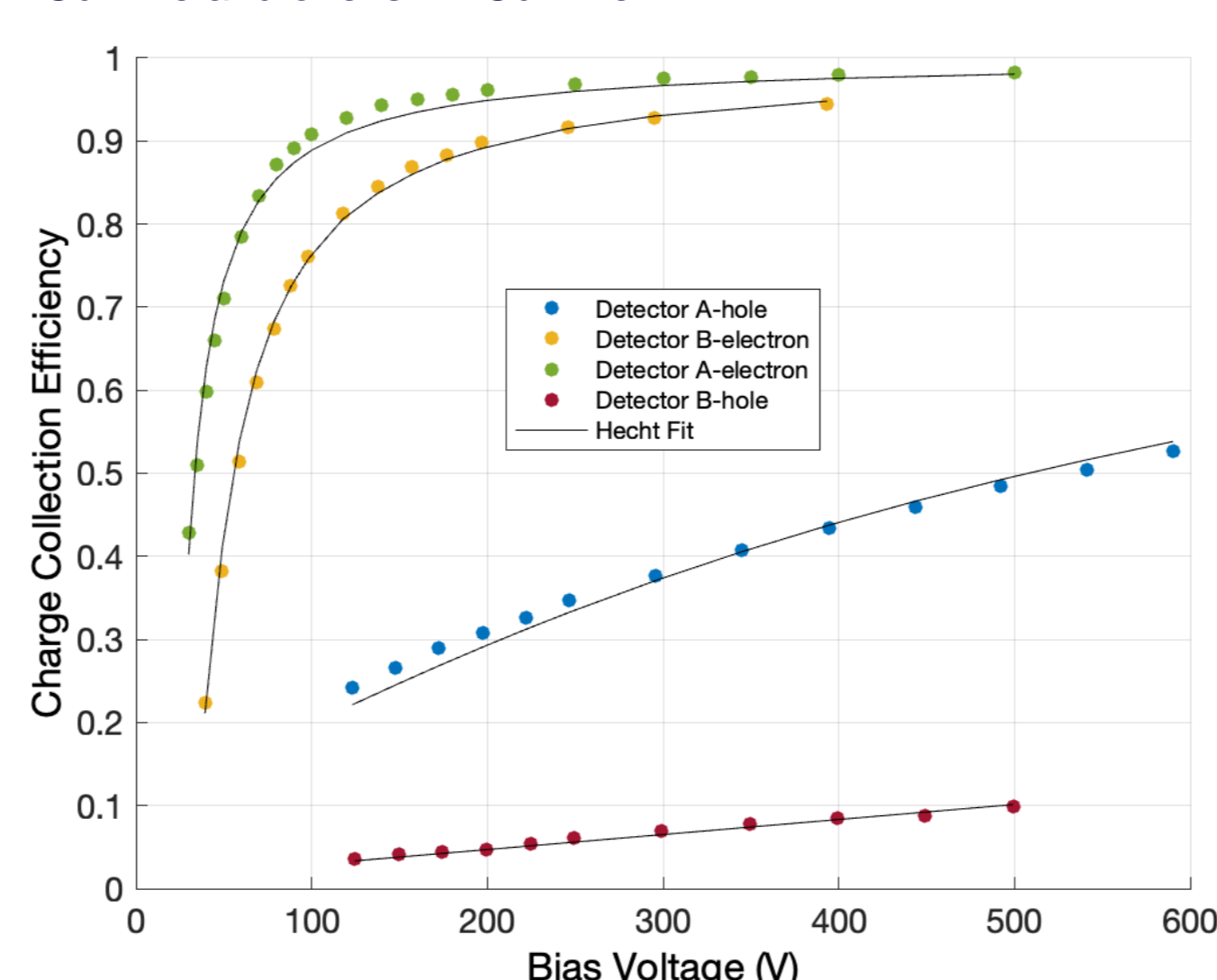
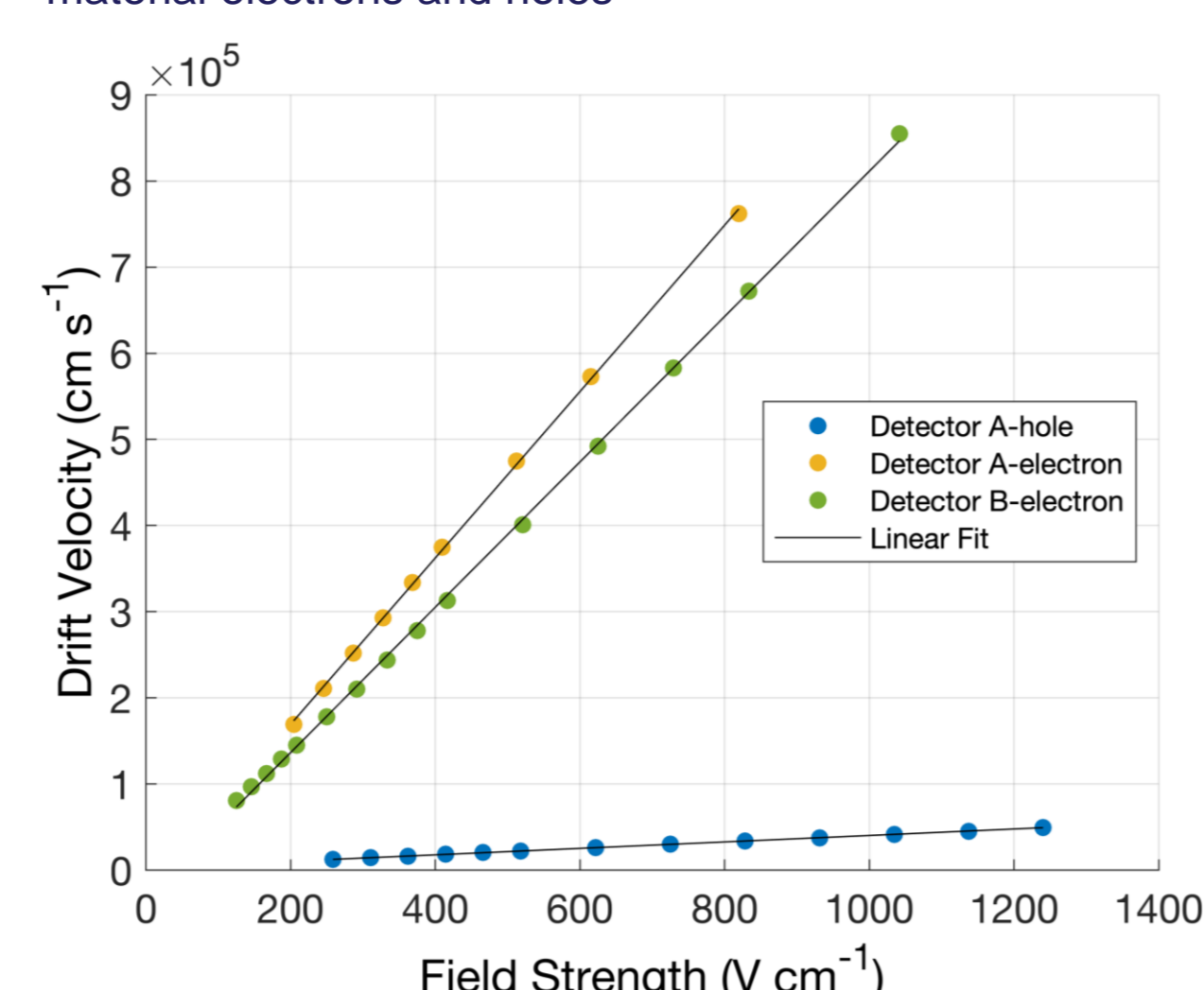


Figure 3: Measured mobilities for both high flux and low flux material electrons and holes



Sample	Type	Electrodes	Fabricated	Thickness (mm)	$\mu_e\tau_e$ ($\times 10^{-3}$ cm ² V ⁻¹ S)	$\mu_h\tau_h$ (cm ² V ⁻¹ S)	τ_e (μ s)	μ_e/τ_e ($\times 10^{-10}$ cm ² V ⁻¹ S ⁻¹)	μ_h (cm ² V ⁻¹ S ⁻¹)	τ_h (μ s)
Detector A	HF	Redlen	2018	5	5.9±0.1	990±20	6.0	2.4±0.1	38±3	6.2
Detector B	LF	Redlen	2018	5	1.2±0.1	840±12	14.4	0.4±0.1	-	1.1*
Detector C	HF	Due2lab	2023	2	3.4±0.1	980±11	3.5	1.2±0.1	44±1	2.7
Detector D	HF	Due2lab	2023	2	3.9±0.1	790±15	5.0	1.2±0.1	32±1	3.8

Table 1: (Left) values for mobility and lifetime found from fitting the Hecht equation and linear mobility data. *Calculated using the average hole mobility of Detector A,C and D (38 cm²V⁻¹S⁻¹).

3. Low Temperature Photoluminescence (PL)

To understand a possible cause of the differences in carrier lifetime between LF and HF CdZnTe measured in section 2, each material was cooled to 4 K and illuminated with above-bandgap photons (660 nm). A spectrometer then measured the PL photons. Figure 4 shows a ~50x difference in intensity between the two samples, indicating that a non-radiative process could be occurring in the HF-CdZnTe. The relative peak heights for the A-centre, donor acceptor pair (D,A) and the first and second order phonon replica (LO) have increased in the HF-CdZnTe sample compared to the LF-CdZnTe sample. This is consistent with the changes observed in literature with different concentrations of indium doping. Indium doping compensates for Cd vacancies or residual impurities, reducing trapping centers for holes, and therefore higher indium doping could explain the increase in hole lifetime. This in turn may explain the higher flux capabilities observed in this material [3].

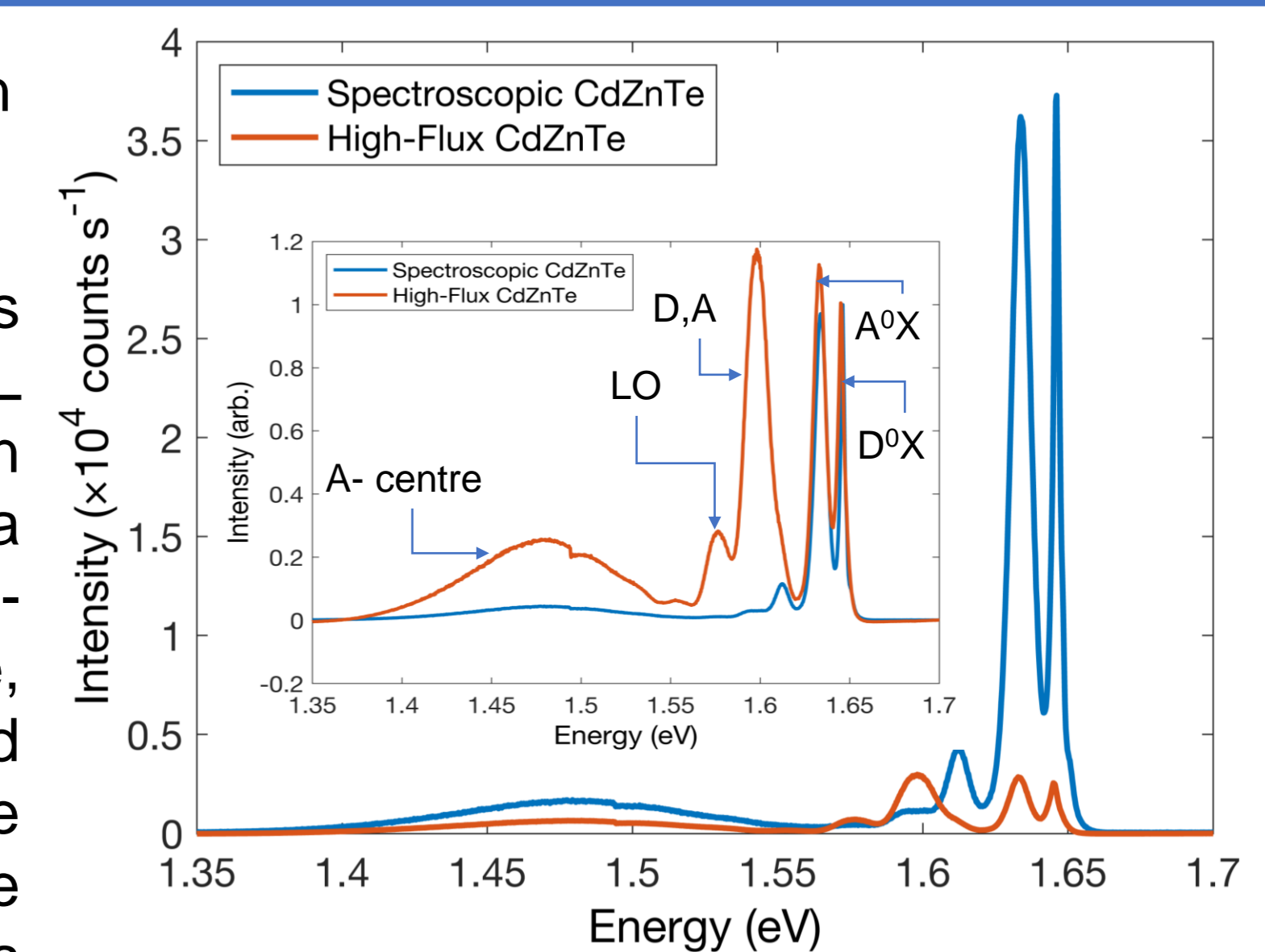


Figure 4: 4K photoluminescence spectrum of HF-CdZnTe and spectroscopic LF-CdZnTe, integration time has been converted into counts per second. (Insert) Spectrum normalised to D⁰X peak. The notch seen at 1.48eV is an artefact due to an image stitching error.

Sample	A-ctr.	P.R.	LO	DAP	A ⁰ X	D ⁰ X	X
HF-CdZnTe	1.479	1.552	1.577	1.598	1.633	1.645	1.648
LF-CdZnTe	1.481	1.575	1.593	1.612	1.634	1.646	1.651

Table 2: Comparison of peak energies between HF-CdZnTe and LF-CdZnTe, in eV \pm 0.0005 eV

4. High Photon Flux Measurement

To confirm the charge carrier properties measured translate to performance at high fluxes, Diamond B16 beamline data was taken using Detector C (see table 1). The detector was exposed to fluxes up to 5.94×10^8 20 keV photons·s⁻¹·mm⁻². The detector was connected to a trans-impedance amplifier and a digitizer with a sampling rate of 200 kHz. This was done to investigate linearity and afterglow effects. Figure 6 (insert) shows linearity up to 5.94×10^8 20 keV photons·s⁻¹·mm⁻² with R² = 0.9996. The decay of the current in the sensors displayed a number of components and accurate fitting was a challenge. A fit to the longer-lived component with a single exponential was made giving a time constant of 31 s. This long-lived afterglow has implications for fast imaging applications based on HF-CdZnTe. The afterglow signal 1 s after X-rays were shut off was calculated as a function of flux, this value was averaged over 2000 data points (10 ms). Afterglow signal decreases sharply with increasing flux to <0.5% of the radiation current at the highest fluxes. This is due to the charge created by X-rays filling traps. As the flux increases, the magnitude of the afterglow tends towards a constant value consistent with 100% of these traps being filled [2].

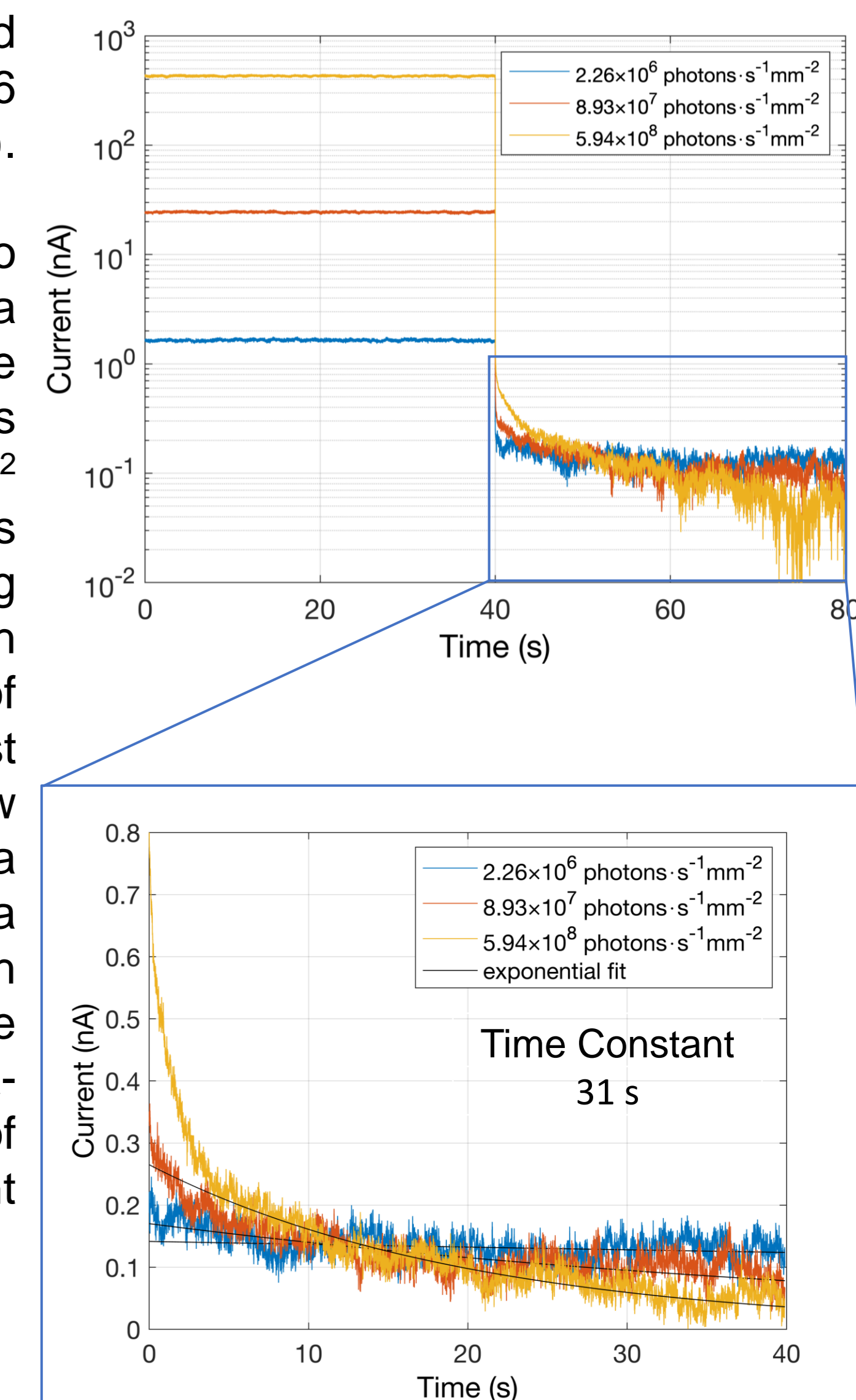


Figure 5: (Top) Trace of flux with time, with three different aluminium beam line attenuators in place to give differing flux values. Fast shutter close centred at 40 s. (Bottom) Residual signal after X-rays are off, single exponential fitted to slow component (10 s after X-ray off) of the data and a time constant of 31 s calculated.

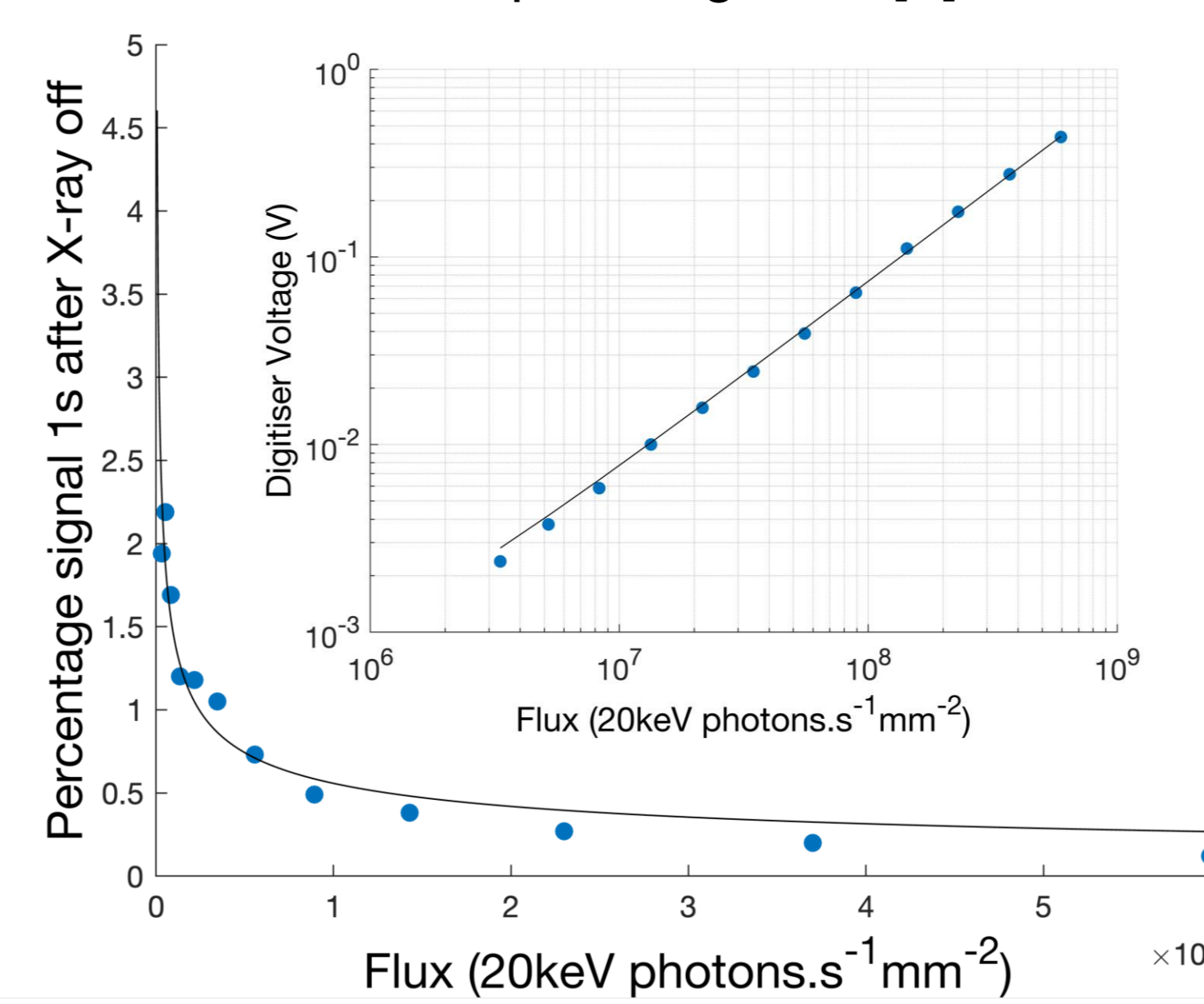


Figure 6: (Left) Percentage of residual signal measured 1s after X-rays are off, compared to the flux level irradiating the detector before the shutter is closed, averaged over 2000 readings (or 10 ms). (Insert) Pad detector digitiser output vs calibrated photon flux using a range of 5.5 mm to 0 mm of aluminium beamline attenuation.

Conclusions

HF-CdZnTe is the most promising sensor material for a new generation of photon light sources but is still relatively poorly understood. Measurements presented here clearly demonstrate a significant improvement in the lifetime of holes compared to low flux CdZnTe. PL measurements demonstrated significant differences between the two materials. Differences in the overall PL intensity and ratio of the characteristic peaks suggests differences in the indium doping concentration in the two materials. The performance of detectors produced from the HF-CdZnTe material were characterised at high fluxes, where it was confirmed that they behaved linearly up to the flux of 5.94×10^8 20keV photons·s⁻¹·mm⁻². Afterglow after X-ray exposure was observed, and had a long lifetime of 31 s.

References

- [1] D. S. Bale and C. Szeles, "Nature of polarization in wide-bandgap semiconductor detectors under high-flux irradiation: Application to semi-insulating Cd_{1-x}Zn_xTe," *Physical Review B, Condensed Matter and Materials Physics*, vol. 77, no. 3, Jan. 2008, doi: 10.1103/physrevb.77.035205.
- [2] O. Baussens, C. Ponchut, M. Ruat, M. Bettelli, S. Zanettini, and A. Zappettini, "Characterization of High-Flux CdZnTe with optimized electrodes for 4th generation synchrotrons," *Journal of Instrumentation*, vol. 17, no. 11, p. C11008, Nov. 2022, doi: 10.1088/1748-0221/17/11/c11008.
- [3] J. Teng et al., "Influence of In dopant on PL Spectra of CdZnTe Crystals," *Journal of the Korean Physical Society*, vol. 53, no. 1, pp. 146-149, Jul. 2008, doi: 10.3938/jkps.53.146.
- [4] B. Thomas, M. C. Veale, M. D. Wilson, P. Seller, A. Schneider, and K. Iniewski, "Characterisation of Redlen high-flux CdZnTe," *Journal of Instrumentation*, vol. 12, no. 12, p. C12045, Dec. 2017, doi: 10.1088/1748-0221/12/12/c12045.
- [5] J. Xia, M. Streicher, Y. Zhu, and Z. He, "Measurement of Electron Mobility-Lifetime product in 3-D Position-Sensitive CDZnTe detectors using the VAD-UMV2.2 Digital Readout system," *IEEE Transactions on Nuclear Science*, vol. 65, no. 11, pp. 2834-2837, Nov. 2018, doi: 10.1109/tns.2018.2876021.